SEE-inducing effects of cosmic rays at the High-Altitude Research Station Jungfraujoch compared to accelerated test data

Z. Török, S. P. Platt and Cai Xiao Xiao
School of Computing, Engineering and Physical Science
University of Central Lancashire
Preston, Lancs. PR1 2HE, England
email: ztorok@ieee.org, spplatt@uclan.ac.uk, xxcai1@uclan.ac.uk

***Abstract*—We analyse the SEE-inducing effects of cosmic rays using scientific CCDs and make direct comparison of results obtained in the natural cosmic ray field at altitude with those from accelerated test in neutron beams.**

***Index Terms*—Charge-coupled devices, cosmic rays, dosimetry, environmental radiation effects, neutron radiation effects, radiation detectors, semiconductor device radiation effects.**

I. Introduction

Charge-coupled devices (CCDs) can be used to image radiation-induced charge deposition [1]–[4]. CCDs provide spatial information about the deposited charge at moderately fine resolution. We have previously shown how CCD data allow the evaluation of neutron single-event effect (SEE) phenomena and enable the SEE-inducing effects of radiation fields to be characterised [5], [6].

In this paper we analyse cosmic-ray induced events captured at the High-Altitude Research Station Jungfraujoch [7] in the Swiss Alps. This provides a natural neutron flux due to cosmic rays which is about 10 times that at mid-latitude sea-level locations. We make direct comparisons between the charge and spatial characteristics of events with equivalent data captured in the neutron beam at the Los Alamos Neutron Science Center (LANSCE) ICE House [8] and undertake a comparative analysis of the two data sets.

Our experiment was colocated with a related but separate experiment using commercial webcams, which was undertaken by our SPAESRANE collaborators MBDA(UK) and which is also presented at this conference [9].

II. Experimental procedure

An imaging SEE monitor (ISEEM) using a Kodak KAF-0402E scientific CCD as the sensing element was deployed in the Sphinx laboratory at Jungfraujoch between January 2006 and April 2007, close to the Jungfraujoch IGY neutron monitor.[1] We describe results obtained over the period from 18 January to 12 September 2006 and from 15 November 2006 to 12 April 2007. Allowing for short interruptions, 374 days' worth of data were gathered and are analysed here.

[1]So called because this neutron monitor design was standardised for the International Geophysical Year 1957.

TABLE I: ISEEM key parameters

sensor	Kodak KAF-0402E
columns	768
rows	512
pixels	393216
pixel size	9 μm
area	31.85 mm^2
fill factor	100 %
pixel charge capacity	16 fC
anti-blooming drain	none[1]
charge resolution	8.3 aC

[1] Anti-blooming correction is possible in post-processing.

The sensor used was a modified version of the same ISEEM sensor described elsewhere [10] and previously used in trials at LANSCE [5]. Key monitor parameters are listed in Table I. Cosmic ray interactions in the CCD lead to detection of charge transients in CCD frames. Such events are detected as contiguous groups of pixels with elevated grey levels. Event processing was as described in [5], including frame cleaning and anti-blooming correction, ensuring that the Jungfraujoch data are directly comparable to those from LANSCE. We took advantage of the relatively low event rate in the natural field by reducing the frame rate to 0.19 s^{-1} and saving three frames around each event (i.e. each frame in which an event is detected and the preceding and following frames). In this way, we retain a complete record of the status of the experiment at the occurrence of each event. The experiment operated automatically under remote control with the support of local custodians at the laboratory.

We exposed two different CCDs during the earlier and later parts of the experiment. We identify these as sample 1 (exposed from January to September 2006) and sample 2 (exposed from November 2006 to April 2007).

III. Neutron environment

Fig. 1 shows the IGY neutron monitor count rate observed during the experiment [11]. The data in Fig. 1 are corrected

978-1-4244-1704-9/07/$25.00 ©2007 IEEE

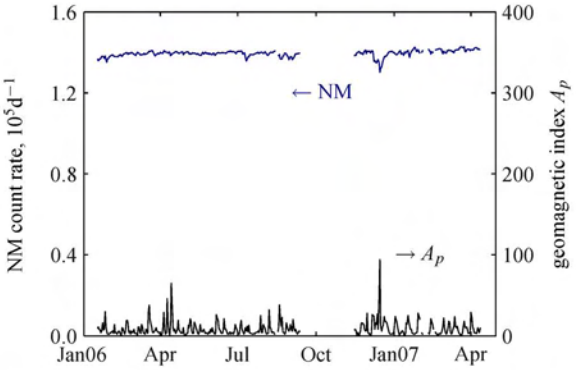

Fig. 1: Cumulative daily pressure-corrected IGY neutron monitor counts at Jungfraujoch, and average daily global geomagnetic index A_p.

for local atmospheric pressure. The rate is largely constant; the slight increase (around 2% over the duration of the experiment) is consistent with the approach to solar minimum in 2007. The effect of a solar particle event in December 2006 is visible as a Forbusch decrease followed by a short-lived (c. 20 min at Jungfraujoch) enhancement of the neutron flux. Fig. 1 also shows the daily average value of the global index of geomagnetic disturbance, A_p [12]. The most significant disturbance (A_p = 94) is associated with the December solar episode.

We determined the neutron spectrum at Jungfraujoch using the online version of the QinetiQ Atmospheric Radiation Model (QARM [13]–[15]). A QARM calculation requires the user to specify a date, to account for large-scale solar modulation of the primary cosmic ray field, and a value of the planetary index, K_p (a nonlinear representation of the A_p index shown in Fig. 1[2]), to account for solar influence on the earth's magnetic field. As indicated in Fig. 1, geomagnetic conditions during the course of this experiment were largely quiet. The median value of K_p was 1+; its inter-decile range was from 0 to 3+. QARM predicts that these variations will not have significantly affected the cosmic neutron flux at Jungfraujoch. QARM also indicates that the effect of solar modulation on the neutron spectrum are slight, predicting a variation of only a few percent over the duration of the experiment. Both results are consistent with the data shown in Fig. 1. Accordingly, the spectrum was calculated for a date close to the midpoint of our experiment using a K_p index close to the median for the experiment, as given in Table II.

The LANSCE spectrum was determined from facility dosimetry during our trials there [16].

Fig. 2 compares spectra for the neutron fields at LANSCE and at Jungfraujoch. We expect ISEEM to be sensitive to neutrons above approximately 2 MeV [17]; we have confirmed its sensitivity to a ^{252}Cf source with a peak neutron flux around 2.5 MeV. QARM predicts an integrated neutron flux above 2 MeV of 6.55×10^{-2} cm^{-2}s^{-1} at

[2] K_p is expressed on a 28-point scale from 0 (quietest, A_p=0) through 0+, 1-, 1 etc. to 9 (most disturbed, A_p=400) [12].

TABLE II: QARM simulation parameters

latitude	46.55°
longitude	7.98°
altitude	3.57 km
incident particles	galactic cosmic rays
date	30 June 2006
K_p	1

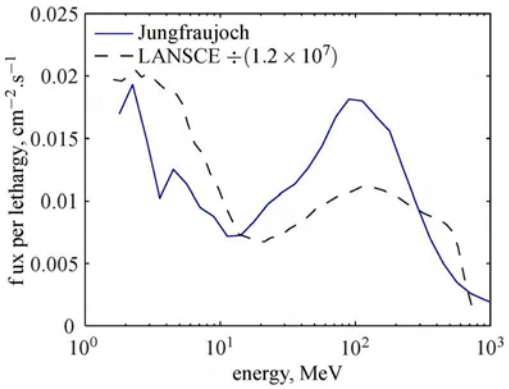

Fig. 2: Neutron spectra at Jungfraujoch and LANSCE

TABLE III: Summary event rates

experiment		duration s	events
Jungfraujoch	1/06 – 9/06	2.03×10^7	405
	9/06 – 4/07	1.18×10^7	211
LANSCE		1206	38272

Jungfraujoch. The corresponding flux observed at LANSCE was 7.82×10^5 cm^{-2}s^{-1}. The LANSCE spectrum in Fig. 2 is therefore divided by the acceleration factor (1.2×10^7) to facilitate a direct comparison. The two spectra are qualitatively similar, although the QARM simulation predicts a lower proportion of the spectrum to be contained in the peak below 10 MeV and a correspondingly greater proportion to be in that above 10 MeV.

IV. Results

A. Raw event rates

Table III shows summary data for events from which at least 8 fC was collected. The average event rate at Jungfraujoch was 1.72 d^{-1} for sample 1, 1.54 d^{-1} for sample 2, 1.66 d^{-1} on average. At LANSCE the event rate was 31.7 s^{-1}. Fig. 3 compares ISEEM event rates at Jungfraujoch to raw count rates from the Jungfraujoch IGY neutron monitor [11]. The NM counts in Fig. 3 are uncorrected for variations in local atmospheric pressure, and therefore show the influence of the varying atmospheric mass above the location of the experiment. We do not observe any correlation between raw NM counts and ISEEM event rates.

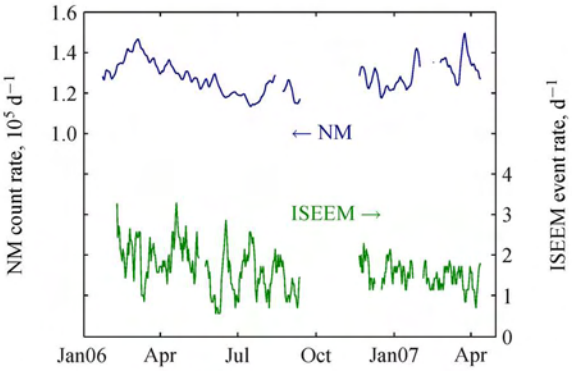

Fig. 3: ISEEM event rate compared to IGY NM count rate (uncorrected for pressure): weekly running averages

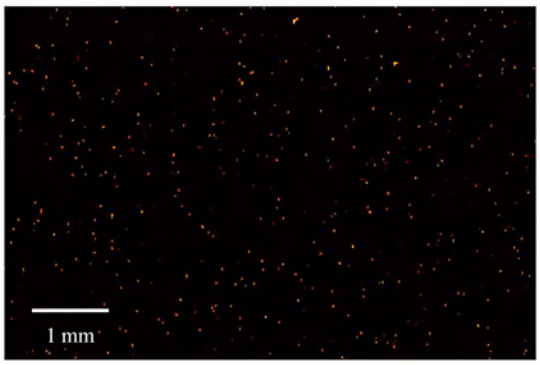

Fig. 4: Montage of events captured at Jungfraujoch

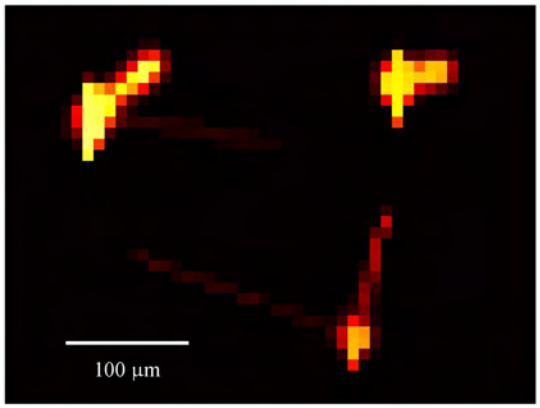

Fig. 5: Example neutron events captured at Jungfraujoch

B. Event characteristics

Fig. 4 shows all 616 events captured at Jungfraujoch in a single montage image without anti-blooming correction. Many events show intense blooming effects caused by charge overspill in vertical direction.

Fig. 5 shows example events selected from the Jungfraujoch data set. Each shows characteristics of neutron interactions in or near the active region of the CCD, leading to the emission of evaporation particles and strong ionisation from the recoiling residual ion. Blooming artefacts are visible at the interaction

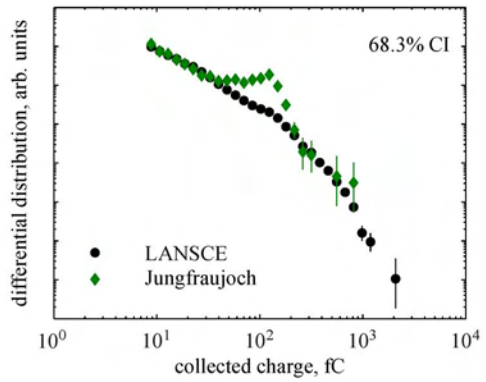

Fig. 6: Differential charge-collection spectra at Jungfraujoch and LANSCE

sites where the generated charge density exceeds the pixel capacity.

For example, the event shown at top left of Fig. 5 is the largest (in terms of collected charge) observed during the trial. In total 0.8 pC was collected from this interaction. To the right, an ionising particle travels approximately 80 μm in the plane of the array, depositing approximately 7.6 MeV 0.34 pC as it does so. To the lower right a light particle with stopping power 4.7 keV μm^{-1} travels approximately 160 μm before leaving the detector active volume. This is consistent with the emission of a proton with energy around 20 MeV and range 2.4 mm in silicon. The residual heavy ion deposits 9.8 MeV in a short distance leading to blooming as the pixel charge capacity is exceeded.

Fig. 6 compares charge-collection spectra for events captured at Jungfraujoch and at LANSCE. Vertical bars show 68.3% confidence intervals. The data are are normalised over the region from 8 fC to 32 fC. Above this region, between about 40 fC (1.1 MeV) and about 200 fC (4.5 MeV), the Jungfraujoch data are elevated above the LANSCE data. The peak of the Jungfraujoch data is at about 130 fC (3 MeV). This anomaly seems to be due to radioactive contamination of the CCD or its package. This issue is considered further in section IV-C, below. From the data in Fig. 6 we can estimate that approximately 64% of the events observed in the Jungfraujoch data set may be due to contamination. This corresponds to about one such event per day – insignificant in an accelerated test context. Outside the anomalous region, the atmospheric data show a substantially similar spectrum to that obtained in accelerated tests.

Fig. 7 shows a subset of events from the anomalous region. Most events in this region are consistent with direct ionisation from a charged particle such as an α particle entering the CCD from above. Several of these events exhibit blooming; this can occur when a sufficiently energetic particle stops near the top of the CCD active volume, depositing all its energy within a single pixel and exceeding the pixel capacity of 16 fC (0.36 MeV). From the LANSCE and Jungfraujoch charge-collection spectra (Fig. 6) we estimate that 25% of these events are true neutron-induced events that 75% are due

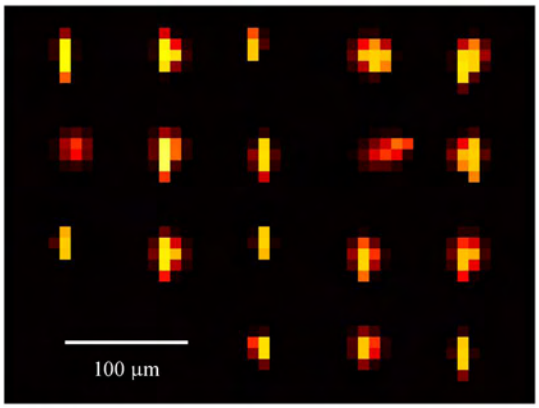

Fig. 7: Example events from the anomalous region at Jungfraujoch

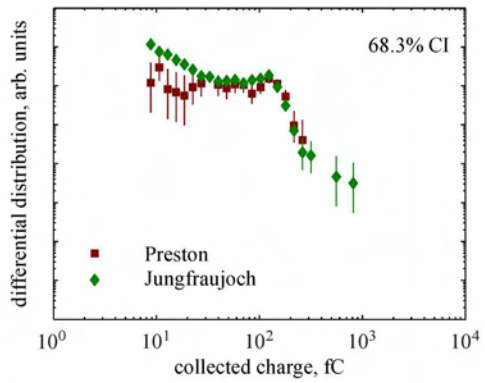

Fig. 8: Differential charge-collection spectra at Jungfraujoch and Preston. The latter is almost wholly due to contaminants

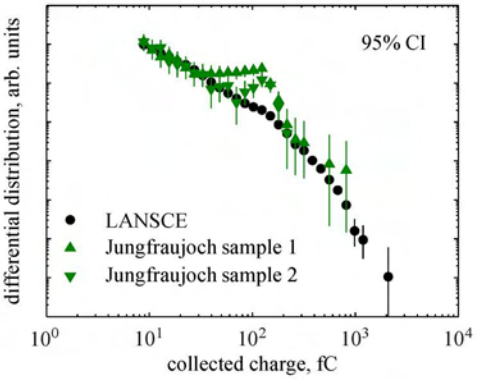

Fig. 9: Differential charge-collection spectra showing the difference between the two samples deployed at Jungfraujoch

to contamination.

C. *Influence of radioactive contamination*

We also investigated event rates in our laboratory in Preston (53.76° north, 2.72° west, 30 m above mean sea level). Based on the observation of 75 events we determine an event rate of $1.15 \times 10^{-5}\,\mathrm{s}^{-1}$ ($0.99\,\mathrm{d}^{-1}$) $+13\%/-12\%$ standard uncertainty, consistent across a small set of CCDs. The neutron flux at Preston is reduced from that at Jungfraujoch by a factor of ten; we estimate that at least 90% of the events in the Preston data set are due to contaminants. This is consistent with the excess event rate estimated from the charge-collection spectra in Fig. 6.

Fig. 8 shows the charge-collection spectrum from this data set of supposed contaminant events, in comparison to that from Jungfraujoch. The data in Fig. 8 are normalised between 100 fC and 200 fC. The maximum charge collected from an event at Preston was 247 fC, corresponding to an energy of 5.6 MeV. The peak of the distribution occurs at about 130 fC (3 MeV). These results are consistent with trace radioactive contamination of the CCD packaging, perhaps from the cover glass, as described by McColgin et al. [18] who detected uranium and thorium contaminants in cover glasses used in Kodak CCDs. Such contaminants emit α articles in the energy range from 4 MeV to 9 MeV [19]. Each device used in our experiment had a fixed cover glass approximately 1 mm above the CCD. This leads to a maximum possible deposited energy in the CCD of approximately 8 MeV, allowing for energy losses predominately in the CCD overlayer. The cover glass is about 1 mm thick; losses in the cover glass would lead to a low-energy continuum in the contaminant spectrum, as we observe in the Preston data shown in Fig. 8.

We note that McColgin et al. [18] investigated several types of cover glass and detected α particles at rates $1\,\mathrm{d}^{-1}$ (for "low-α" glass), $8\,\mathrm{d}^{-1}$ and $16\,\mathrm{d}^{-1}$ in a CCD with active area $2.43\,\mathrm{cm}^2$. Our rate of $1\,\mathrm{d}^{-1}$ in $0.32\,\mathrm{cm}^2$ is consistent with the rate observed from their "glass A".

Comparing the Preston and Jungfraujoch data two features are noticeable. First, the excess charge distribution at Jungfraujoch is similar to that which we attribute to radioactive contamination; secondly, there are statistically significant differences between the behaviour of the two samples in this region, as illustrated in Fig. 9. It is likely to reflect the presence of a different mix or distribution of contaminants in the CCD cover glasses, and accounts for the observed difference in event rates between the two devices.

Fig. 10 presents contour plots showing the distribution of events versus charge and event area. The data in Fig. 10 are corrected for blooming [5]. The distribution of events at LANSCE (due to neutrons), Preston (supposed to be mostly due to contaminants) and Jungfraujoch are shown. The contours show differential distributions at LANSCE and Jungfraujoch, normalised between 8 fC and 32 fC in each case. The points show the locations of events observed at Preston. Fig. 11 illustrates the distribution of excess events at Jungfraujoch. This closely matches the distribution of events observed at Preston. We can identify a region within which most of the excess events occur and which can be used to exclude the majority of these. Such a region is shown by the solid line in Fig. 11. This region contains 89% of the Preston dataset, 52% of the Jungfraujoch dataset and 12% of the LANSCE dataset. A filter defined by excluding events in this region removes most of the contaminant events at the

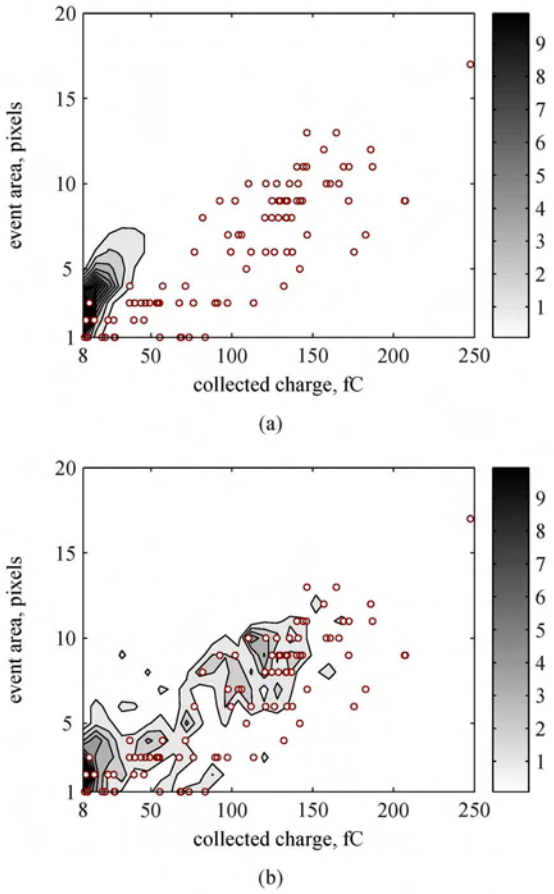

Fig. 10: Event distributions versus charge and area. Scatter points show events observed at Preston. Contours show differential distributions at LANSCE (a) and Jungfraujoch (b). The scale is arbitrary; normalisation is between 8 fC and 32 fC in each case.

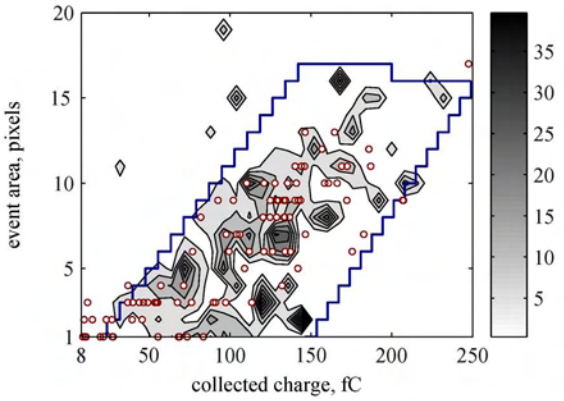

Fig. 11: Distribution of excess events at Jungfraujoch. The scale shows the ratio of the Jungfraujoch distribution to that at LANSCE. The locations of events at Preston are also shown. Most of these are enclosed by the boundary shown.

expense of removing some of the true neutron-induced event set. Filtering the event dataset to exclude those in the boundary

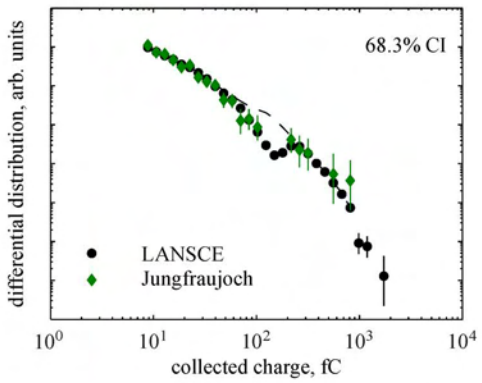

Fig. 12: Differential charge-collection spectra at Jungfraujoch and LANSCE after filtering as shown in Fig.11

results in the differential charge collection spectra shown in Fig. 12. Fig. 12 shows that outside the contaminant region the charge collection spectra are consistent between Jungfraujoch and LANSCE, indicating that the charge-inducing behaviour of the two neutron fields are comparable.

V. Discussion

The apparently anomalous region which we observe in our Jungfraujoch data set appears to be consistent with radioactive contamination of the CCD or its package. We think this is likely to be thorium or uranium contaminants of the glass forming the CCD cover slip. Naturally occurring uranium and thorium isotopes with long half-lives are known to emit alpha particles with energies between 4 MeV and 9 MeV and to be present in trace quantities in many glasses, leading to background signals in applications including photomultiplier tube detectors and CCDs [18], [20]. We are currently investigating these effects by undertaking exposures of CCDs with and without cover glasses.

We have attempted to identify and remove contaminant events based on the spatial distribution of induced charge. We have applied anti-blooming correction and an exclusion filter in collected area and charge to do so. This is incompletely effective in removing contaminant effects, and also removes some true neutron-induced events. However, it does demonstrate that the distributions of Jungfraujoch and LANSCE event characteristics are well matched outside the region in which contaminant events occur, giving confidence that the LANSCE field provides a fair representation of the majority of SEE effects observed in the natural cosmic ray field. Although this is unsurprising, we believe our work to provide the first direct experimental evidence.

It is unlikely than an image processing approach can unambiguously identify contaminant events, not least because the observed phenomena (emission of α particles) is also a possible result of neutron interactions. Nonetheless, knowledge of the rate of occurrence and the distribution of contaminant effects allows these to be treated statistically.

Charge-collection characteristics imply that 64% of the events observed at Jungfraujoch were due to contamination.

On that basis we determine a mean rate of cosmic-ray induced events at Jungfraujoch which is approximately $0.6\,d^{-1}$ ($0.025\,h^{-1}$). The corresponding rate at LANSCE is approximately $1 \times 10^5\,h^{-1}$, representing an acceleration factor of 4×10^6. This is somewhat lower than predicted by QARM 1.2×10^7 – that is, the event rate at Jungfraujoch is somewhat greater than predicted. The prediction assumes a constant event cross-section above 2 MeV – that is, it is based on integral neutron flux above this energy. This is likely to be a slight overestimate. For example, the ratio of integral neutron flux above 2 MeV is slightly less (9.3×10^6). The events at Jungfraujoch might be enhanced slightly by other constituents of cosmic ray showers, although QARM predictions indicate that neutrons should dominate strongly.

In the longer term we also hope to expose similar monitors in this and other locations, including at high altitude and high latitude, to investigate event rate variations. A dataset of the order of 10 000 such events would be useful for benchmarking accelerated test data; such a data set would require an exposure of around $6400\,cm^2 \cdot d$ under comparable conditions to those experienced in this work. This could be achieved with an exposure of around a year using either a single CCD with a sufficiently large area ($14\,cm^2$) or several smaller devices.

VI. Conclusion

We have successfully performed experiments at high altitude using an imaging SEE monitor based on a scientific CCD to measure the effects of the natural cosmic neutron environment. We have compared results with equivalent data gathered during exposure to a high-energy, high-flux neutrons beam as used for accelerated testing for SEE. We are able to demonstrate that the detailed characteristics of interactions are similar in the two fields, and to determine an acceleration factor applicable to accelerated testing for SEE. Our work provides validation data both for comparison between accelerated and system soft error rate measurements and also for atmospheric radiation modelling.

Acknowledgements

This work was supported by the UK Department of Trade and Industry and BAE SYSTEMS under the Solutions for the Preservation of Aerospace Electronic Systems Reliability in the Atmospheric Neutron Environment (SPAESRANE) project (www.spaesrane.com).

The authors gratefully acknowledge that the International Foundation High Altitude Research Stations Jungfraujoch and Gornergrat (HFSJG), 3012 Bern, Switzerland, made it possible for us to carry out our experiments at the High Altitude Research Station at Jungfraujoch. We should also like to thank the research station custodians, Mr. and Mrs. Fischer and Mr. and Mrs. Hemund, for their support to our activities. Jungfraujoch neutron monitor data were kindly provided by the Cosmic Ray Group, Physikalisches Institut, University of Bern, Switzerland.

References

[1] R. Bailey, C. J. S. Damerell, R. L. English, A. R. Gillman, A. L. Lintern, S. J. Watts, and F. J. Wickens, "First measurements of efficiency and precision of CCD detectors for high energy physics," *Nucl. Inst. Meth. Phys. Res.*, vol. 213, no. 2-3, pp. 201–215, Aug. 1983.

[2] T. S. Lomheim, R. M. Shima, J. R. Angione, W. F. Woodward, D. J. Asman, R. A. Keller, and L. W. Schumann, "Imaging charge-coupled device (CCD) transient response to 17 and 50 MeV proton and heavy-ion irradiation," *IEEE Trans. Nucl. Sci.*, vol. 37, no. 6, pp. 1876–1885, Dec. 1990.

[3] G. J. Yates, G. W. Smith, P. Zagarino, and M. C. Thomas, "Measuring neutron fluences and gamma/X-ray fluxes with CCD cameras," *IEEE Trans. Nucl. Sci.*, vol. 39, no. 5, pp. 1217–1225, Oct. 1992.

[4] A. M. Chugg, R. Jones, P. Jones, P. Nieminen, A. Mohammadzadeh, M. S. Robbins, and K. Lovell, "CCD miniature radiation monitor," *IEEE Trans. Nucl. Sci.*, vol. 49, no. 3, pp. 1327–1332, Jun. 2002.

[5] Z. Török and S. P. Platt, "Application of imaging systems to characterization of single-event effects in high-energy neutron environments," *IEEE Trans. Nucl. Sci.*, vol. 53, no. 6 part 1, pp. 3718–3725, Dec. 2006.

[6] S. P. Platt and Z. Török, "Analysis of SEE-inducing charge generation in the neutron beam at The Svedberg Laboratory," *IEEE Trans. Nucl. Sci.*, vol. 54, no. 4, pp. 1163–1169, Aug. 2007.

[7] Hochalpine Forschungsstation Jungfraujoch. [Online]. Available: http://www.ifjungo.ch

[8] B. Takala and S. A. Wender. Accelerated neutron testing of semiconductor devices. [Online]. Available: http://wnr.lanl.gov/see/poster.pdf

[9] A. M. Chugg, A. J. Burnell, and R. Jones, "Webcam observations of SEE events at the Jungfraujoch research station," in *Proc. 9th European Conf. Rad. Effects. Compon. Syst. (RADECS 2007)*, Sep. 2007, paper PD-1.

[10] S. P. Platt, B. Cassels, and Z. Török, "Development and application of a neutron sensor for single event effects analysis," *J. Phys.: Conf. Ser.*, vol. 15, pp. 172–176, Sep. 2005. [Online]. Available: http://stacks.iop.org/1742-6596/15/172

[11] Cosmic Ray Group of the University of Bern. [Online]. Available: http://cosray.unibe.ch

[12] Indices of global geomagnetic activity. GeoForschungsZentrums Potsdam. [Online]. Available: http://www.gfz-potsdam.de/pb2/pb23/niemegk/kp_index

[13] F. Lei, S. Clucas, C. Dyer, and P. Truscott, "An atmospheric radiation model based on response matrices generated by detailed Monte Carlo simulations of cosmic ray interactions," *IEEE Trans. Nucl. Sci.*, vol. 51, no. 6, pp. 3342–3451, Dec. 2004.

[14] F. Lei, A. Hands, S. Clucas, C. Dyer, and P. Truscott, "Improvement to and Validations of the QinetiQ Atmospheric Radiation Model (QARM)," *IEEE Trans. Nucl. Sci.*, vol. 53, pp. 1851–1858, Aug. 2006.

[15] QinetiQ Atmospheric Radiation Model (QARM). [Online]. Available: http://geoshaft.space.qinetiq.com/qarm

[16] B. E. Takala, Nov. 2005, personal communication.

[17] Y. Yahagi, E. Ibe, Y. Takahashi, Y. Saito, A. Eto, M. Sato, H. Kameyama, M. Hidaka, K. Terunuma, T. Nunomiya, and T. Nakamura, "Threshold energy of neutron-induced single event upset as a critical factor," in *Proc. 42nd Annual IEEE International Reliability Physics Symposium*. IEEE, 2004, pp. 669–670.

[18] W. C. McColgin, C. Tivarus, C. C. Swanson, and A. J. Filo, "Bright-pixel defects in irradiated CCD image sensors," in *Semiconductor Defect Engineering - Materials, Synthetic Structures and Devices II, MRS Symp. Proc*, vol. 994, 2007, paper 0994-F12-06.

[19] *Measurement and Reporting of Alpha Particle and Terrestrial Cosmic Ray-Induced Soft Errors in Semiconductor Devices*, JEDEC Solid State Technology Association Std. JESD89A, Oct. 2006. [Online]. Available: http://www.jedec.org/download/search/jesd89a.pdf

[20] P. Theodorsson, "K/Th/U in photomultiplier tubes and improved low-level NaI detectors," *Nucl. Inst. Meth. Phys. Res., A*, vol. 506, pp. 143–148, 2003.